

Reduced Plasma Frequency Calculation Based on Particle-In-Cell Simulations

Tarek Mealy¹, Robert Marosi¹, and Filippo Capolino^{1,2}

(1) Department of Electrical Engineering and Computer Science, University of California, Irvine, CA 92697, USA

(2) Department of Communications and Signal Theory, University Carlos III of Madrid, Spain

tmealy@uci.edu, rmarosi@uci.edu, and f.capolino@uci.edu

Abstract—We propose a scheme to calculate the reduced plasma frequency of a cylindrical-shaped electron beam flowing inside of a cylindrical tunnel, based on results obtained from Particle-in-cell (PIC) simulations. In PIC simulations, we modulate the electron beam using two parallel, non-intercepting, closely-spaced grids which are electrically connected together by a single-tone sinusoidal voltage source. The electron energy and the beam current distributions along the length of the tunnel are monitored after the system is operating at steady-state. We build a system matrix describing the beam's dynamics, estimated by fitting a 2×2 matrix that best agrees with the first order differential equations that govern the physics-based system. Results are compared with the theoretical Branch and Mihran model, which is typically used to compute the plasma frequency reduction factor in such systems. Our method shows excellent agreement with the theoretical model, however, it is also general. Our method can be potentially utilized to determine the reduced plasma frequencies of electron beams propagating in differently-shaped beam tunnels, where no theoretical model yet exists, such as the case of a cylindrical or elliptical electron beam propagating inside of a metallic beam tunnel of cylindrical, square, or elliptical cross-section. It can be applied also to electron beams composed of multiple streams.

Index Terms—Plasma frequency, particle-in-cell (PIC), electron beam, exceptional points, degeneracy.

I. INTRODUCTION

The plasma frequency concept originates from the fact that an infinite cloud of electrons with volumetric charge density ρ_v oscillates at a plasma frequency $\omega_p = \sqrt{\eta\rho_v/\epsilon_0}$ when any electron in the cloud is perturbed from its equilibrium position, where η is the charge-to-mass ratio of an electron and ϵ_0 is the permittivity of free space [1]. Plasma oscillations in linear electron beams are induced by space-charge fields, as explained in [2] and Ch. 9 of [3], which result in repulsive longitudinal forces between charges. However, the calculation of the plasma frequency for a linear stream of charges with finite cross-section requires the consideration of the radial variation of the space-charge fields, electron velocities, and volume charge densities within the beam cross section. Such parameters will fringe, or decay, with radial distance away from the beam center due to the boundary between a beam of finite cross-section and surrounding vacuum, as well as

the presence of the beam tunnel's conducting walls where the longitudinal electric field vanishes. The electronic wave theory for linear beam tubes was developed by Hahn [4] and refined by Ramo [5], utilizing the solutions of Maxwell's equations with corresponding boundary conditions to directly compute the reduced plasma frequency of an electron beam that has a finite cross section and is contained within a cylindrical metallic tunnel. Branch and Mihran further built upon Ramo's work and introduced the plasma frequency reduction factor term, R for cases of both solid and annular electron beams propagating within cylindrical metallic tunnels [6]. It was found that an electron beam with finite cross section will have a plasma frequency that is reduced compared to that of an electron beam with infinite cross section and with the same volumetric charge density. Thus, the reduced plasma frequency is expressed as $\omega_q = R\omega_p$, where $0 < R < 1$. The reduced plasma frequency is one of the fundamental parameters that affects the dispersion characteristics of the so-called space-charge wave or electronic waves, as explained in [5], [2], Ch. 9 in [3], and Ch.9 in [7], which are the waves within the electron beam that possess both velocity and charge modulation in space and time. A linear stream of electrons with average speed u_0 supports multiple space-charge waves with wave function $e^{j\omega t - jkz}$. Typically, there are two dominant charge waves with approximate wavenumbers $k = (\omega \pm \omega_q)/u_0$ [5], [2]. Further theoretical effort was done in works [8], [9], where the authors came up with closed-form formulas to find the plasma frequency reduction factor without numerically solving Branch and Mihran's transcendental equation for the parameter T within the electron beam.

The plasma frequency reduction factor R is one of the fundamental design parameter in electron beam devices since it affects synchronization. As a consequence, the value of R affects the frequency of peak gain in traveling wave tube amplifiers modeled by Pierce theory. Additionally, the choice of drift-tube length between cavities in klystrons for optimal extraction of energy from the modulated electron beam depends on accurate computation of the reduced plasma frequency [5]. The accurate calculation of R is necessary for the modeling and designing of TWTs. For instance, the famous classical theory developed by Pierce requires the calculation of the reduced plasma frequency in order to calculate the parameter $4QC^3 = \omega_q^2/\omega^2$ [10], Ch. 10 in [7], Ch. 12 in [3], which is necessary to accurately calculate the gain. However, the

This material is based upon work supported by the Air Force Office of Scientific Research award number FA9550-18-1-0355 and by the MURI Award number FA9550-20-1-0409 administered through the University of New Mexico.

theoretical calculation of the reduced plasma frequency loses accuracy when the tunnel geometry is different from a circular cylinder or when the electron beam has a cross section that is not circular or annular. The reduced plasma frequency for beams in complex tunnel structures such as a cylindrical beam in folded or helical waveguide is approximated in many works by assuming that the tunnel is cylindrical, i.e., by neglecting the structure periodicity and deformations in the shape of the cylindrical tunnel due to the slow wave structure geometry. Some authors have previously provided a formulation to determine the reduced plasma frequency of an electron beam propagating within a helix slow-wave structure approximated using the sheath helix model, as in [9]; this formulation has been used in TWT modeling software such as CHRISTINE and LMsuite [11], [12]. However, it is not trivial to compute R using the sheath helix model, and most authors studying linear beam tubes simply use the values for R from the Branch and Mihran model [13]–[15]. Furthermore, experimental work has also been performed in [16], [17] aiming at determining the reduced plasma frequency in linear beam tubes. To date, there is a lack of literature available to provide a robust method that can be easily used to verify or find the reduced plasma frequency in complex structures.

In this paper, we present a method that is more general than the Branch and Mihran model (which only yields real-valued space charge wavenumbers) and is rather simple to use. We model the electron beam dynamics by finding the system matrix that describes the small-signal evolution of the electron beam with position and time. The method is similar to the one presented in [18] that was applied to traveling wave tubes. Here, the method is applied to find the eigenmodes of the space-charge waves in a beam tunnel, i.e., waves that do not interact with a propagating electromagnetic mode in a slow wave waveguide. The presented method is based on defining and then finding the system matrix through the interpretation of data extracted from particle-in-cell (PIC) simulations. After the system matrix is determined, we then calculated the two charge-wave wavenumbers. The reduced plasma frequency of the electron beam is inferred by finding the deviation of the two space charge wavenumbers from the average electronic phase constant $\beta_0 = \omega/u_0$.

The purpose of this paper is to show how the proposed method based on three-dimensional PIC simulations is used to calculate the complex wavenumbers of the space-charge waves supported by an electron beam. Since this is the first time we apply the proposed method to the study of the reduced plasma frequency, we apply it to the case of a circular cylindrical beam within a circular cylindrical tunnel, i.e., the case where the solution is known from a previously developed analytical method [5], [6], [8]. In other words, the scope of this paper is to show that the proposed method works for a simple configuration; hence it is a good candidate to study even more complicated configurations where there is no known analytical solution for the plasma frequency reduction factor, such as the case of a two-stream electron beam propagating within a metallic structure that can exhibit growing space charge waves

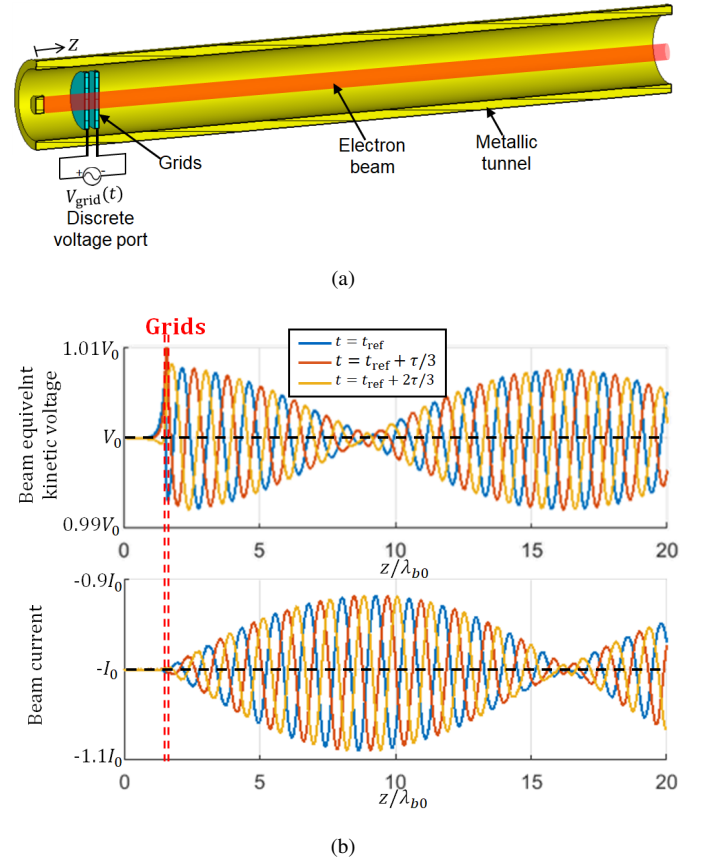


Fig. 1. (a) Setup for PIC simulation used to determine the reduced plasma frequencies of the electron beam in a cylindrical tunnel. Modulating grids are simulated as perfect electric conductors which are transparent to particles. (b) An example of the distribution of the electron beam total (dc and ac) equivalent kinetic voltage, defined as $v_b^{tot}(z, t) = V_0 + v_b(z, t)$ with dc equivalent kinetic voltage V_0 and ac equivalent kinetic voltage $v_b(z, t)$ under the small-signal approximation, and current $i_b^{tot}(z, t) = -I_0 + i_b(z, t)$, calculated based on particles' data exported from PIC simulations at steady state, showing the space-time modulation in the beam voltage and current with respect to arbitrary reference time t_{ref} , where τ is the period of the sinusoidal excitation and λ_{b0} is the average electronic wavelength. The knowledge of the electron beam voltage and current is then used to estimate the 2×2 system matrix \mathbf{M} that describes the differential equation governing the beam dynamics. Finally, the system matrix is used to find the wavenumbers of space-charge waves and consequently the reduced plasma frequency.

(complex space charge wavenumbers) due to the two-stream instability effect [19]–[21]. Motivated by previous work on two-stream instability amplifiers, Islam et al., [22], [23] have proposed a method to generate a two-stream electron beam with two different energies from a single-cathode potential. Our PIC-based model may be useful also to determine the complex space charge wavenumbers in such a configuration. Additionally, our PIC-based model may also be used to study the space-charge wavenumbers for electron beams which interact with lossy materials, such as the case of the resistive wall amplifier [24]–[27].

II. PIC-BASED METHOD

The electron beam has equivalent kinetic dc voltage and dc current V_0 and I_0 , respectively, where the dc equivalent kinetic voltage in the non relativistic case is $V_0 = u_0^2/(2\eta)$

and u_0 is the electrons time-averaged speed, c is the free space speed of light, and $\eta = e/m$ is the charge to mass ratio and e is the electron charge represented as positive number. The magnetically-confined electron beam has a circular cross-section with radius R_b , and is flowing within a metallic cylindrical tunnel with radius R_t , as illustrated in Fig. 1(a). We introduce modulation to the beam using two closely-spaced grids that are made of fictitious metal that is transparent to electrons, i.e., it allows electrons to pass through the grid without being intercepted, while preserving other properties a perfect electrical conductor. The gap between the two grids is chosen to be very small compared to wavelength $d_{grid} \ll \lambda_0$ to have a uniform electric field distribution along the gap and to avoid the transit-time effects for electrons. We apply an ac voltage V_{grid} with a monochromatic sinusoidal signal between the grids in order to generate an axial electric field that modulates the beam in a simple and reproducible way. We rely on three-dimensional PIC simulations implemented in CST Particle Studio to satisfy the equations for charged particles motion and Maxwell equations, which are discretized in space and time in the PIC software.

The PIC solver calculates the instantaneous speed $u_b^{tot}(z, t) = u_0 + u_b(z, t)$, and location of discrete charged macroparticles, where $u_b(z, t)$ represents the ac component of velocity. We represent the total (including dc and ac parts) equivalent kinetic voltage of a non relativistic electron beam using a one dimensional (1D) function as $v_b^{tot}(z, t) = [u_b^{tot}(z, t)]^2 / (2\eta)$ which is expressed as $v_b^{tot}(z, t) = V_0 + v_b(z, t)$, where $v_b(z, t) \approx u_0 u_b(z, t) / \eta$ represents the ac modulation function. Analogously, the total beam current is $i_b^{tot}(z, t) = -I_0 + i_b(z, t)$, where $i_b(z, t)$ represents the ac modulation function, as was done in [18]. Note that the method can be applied also to relativistic beams when using $V_0 = c^2 / \eta \left(\sqrt{1 - (u_0/c)^2} - 1 \right)$ and $v_b^{tot}(z, t) = c^2 / \eta \left(\sqrt{1 - (u_b^{tot}/c)^2} - 1 \right)$, and the ac part is defined as $v_b(z, t) = v_b^{tot}(z, t) - V_0$. However relativistic beams are not considered in this paper and the accuracy of the presented method in those cases is left to future studies.

We define a state vector that describes the ac electron beam velocity and current dynamics as

$$\psi(z, t) = [v_b(z, t), \quad i_b(z, t)]^T. \quad (1)$$

We show in Fig. 1(b) an example of the distribution of the electron beam total (ac and dc) equivalent kinetic voltage and current calculated based on the particle's data exported from PIC simulations at steady state showing the modulation in the beam voltage and current due to the grids, where $\lambda_{0b} = u_0/f$.

At steady state, in the small-signal approximation, the state vector is monochromatic with angular frequency ω and therefore it is represented in phasor domain as [18]

$$\Psi(z) = [V_b(z), \quad I_b(z)]^T. \quad (2)$$

Because the problem we consider is uniform in the z -direction (due to confinement of the beam by a strong axial magnetic

field), we assume that the evolution of the electron beam dynamic along the z -direction is described by a first order differential equation as

$$\frac{d\Psi(z)}{dz} = -j\mathbf{M}\Psi(z), \quad (3)$$

where \mathbf{M} is the 2×2 system matrix and the $e^{j\omega t}$ time dependence is assumed.

The state vector is calculated from the data exported from PIC simulation as done in [18]. We calculate the state vector at discrete locations $\Psi(z = n\Delta_s) = \Psi_n$, where $n = 0, 1, \dots, N$, Δ_s is chosen to be a small position step size ($\Delta_s \leq \lambda_{0b}/3$ and $\lambda_{0b} = u_0/f$), and $N\Delta_s$ is the total length of the structure. According to (3), the sampled state vector should satisfy the relations

$$\Psi_2 = \mathbf{T}\Psi_1, \quad (4.1)$$

$$\Psi_3 = \mathbf{T}\Psi_2, \quad (4.2)$$

$$\vdots$$

$$\Psi_{N+1} = \mathbf{T}\Psi_N, \quad (4.N)$$

where $\mathbf{T} = e^{-j\mathbf{M}\Delta_s}$ is the transfer matrix, \mathbf{M} is related to \mathbf{T} as $\mathbf{M} = j \ln(\mathbf{T}) / \Delta_s$, and the state vectors Ψ_n are calculated directly from PIC simulations.

The relations in (4) represent $2N$ linear equations in 4 unknowns, which are the elements of the transfer matrix \mathbf{T} . Assuming $N > 2$, the system in (4) is mathematically referred to as overdetermined because the number of linear equations ($2N$ equations) is greater than the number of unknowns (4 unknowns). An approximate solution that best satisfies all the given equations in Eq. (4), i.e., minimizes the sums of the squared residuals, $\sum_n \|\Psi_{n+1} - \mathbf{T}\Psi_n\|^2$ is determined like in [18], [28], [29] and is given by

$$\mathbf{T}_{\text{best,approx.}} = (\mathbf{W}_2 \mathbf{W}_1^T) (\mathbf{W}_1 \mathbf{W}_1^T)^{-1}, \quad (5)$$

where

$$\mathbf{W}_1 = [\Psi_1, \quad \Psi_2, \quad \dots \quad \Psi_N], \quad (6)$$

and

$$\mathbf{W}_2 = [\Psi_2, \quad \Psi_3, \quad \dots \quad \Psi_{N+1}], \quad (7)$$

are $2 \times N$ matrices.

Assuming the state vectors take the form of a wave function $\Psi(z) \propto e^{-jkz}$, (3) is simplified to as $k\Psi = \mathbf{M}\Psi$, which constitutes an eigenvalue problem. Therefore, the space-charge waves' wavenumbers are the eigenvalues of \mathbf{M}_{best} ,

$$k = \text{eig}(\mathbf{M}_{\text{best}}), \quad (8)$$

where $\mathbf{M}_{\text{best}} = j \ln(\mathbf{T}_{\text{best}}) / \Delta_s$, which leads to two solutions: k_1 and k_2 . The PIC-based reduced plasma frequency is calculated as $\omega_{q,\text{PIC}} = u_0 \text{Re}(k_2 - k_1) / 2$. The associated "PIC-based" reduction factor calculated as

$$R = \omega_{q,\text{PIC}} / \omega_p \quad (9)$$

where $\omega_p = \sqrt{\eta I_0 / (A u_0 \epsilon_0)}$ and the beam has cross-sectional area $A = \pi R_b^2$.

III. ILLUSTRATIVE EXAMPLE

As an illustrative example, we consider a solid electron beam with equivalent kinetic dc voltage $V_0 = 6.7$ kV (which corresponds to $u_0 = \sqrt{2\eta V_0} = 0.16c$), beam radius $R_b = 0.5$ mm, and the beam current I_0 that is swept. The tunnel is made of a perfect electric conductor and has radius $R_t = 2$ mm and total length of 120 mm. We use two grids spaced apart with a gap of $d_{\text{grid}} = 0.2$ mm and a grid excitation voltage $V_{\text{grid}}(t) = 100 \cos(2\pi ft)$ volts. An axial dc magnetic field of 1 T is used to confine the electron beam. All 3D PIC simulations in this paper are performed using CST Particle Studio. The 3D segmentation performed in CST uses hexahedral mesh with mesh size of approximately $\Delta_{\text{mesh}} = \lambda_{b0}/30 = 0.2$ mm calculated at $f = 10$ GHz, where $\lambda_{b0} = u_0/f$ and $u_0 = 0.16c$. The total number of charged particles used by PIC simulations to model the electron beam is approximately 10^6 particles. We run PIC simulations for a total time of $t_{\text{sim}} = 10$ ns, where the beam dynamics in phasor domain are obtained based on the particles' data on the time period from $t = t_{\text{sim}} - \tau \rightarrow t_{\text{sim}}$, where $\tau = 1/f$ is the period of the applied sinusoidal signal.

We sweep the electron beam dc current I_0 at constant frequency of $f = 5$ GHz. We show in Fig. 2(a) the ‘‘PIC-based’’ dispersion relation for the space-charge wave showing the complex-valued wavenumbers k_1 and k_2 for the two space-charge modes versus beam current, calculated as the eigenvalues for the system matrix obtained based on PIC simulations, \mathbf{M}_{best} . Since we have lossless metals and vacuum in this example, the small imaginary part ($|\text{Im}(k)/\text{Re}(k)| < 10^{-3}$) of the wavenumbers shown in Fig. 2(a) may be attributed to numerical error in our PIC-based method. The method used to find the theoretical wavenumber (dashed-black curves in Fig. 2(a)) is based on the work by Branch and Mihran [6], which gives purely real wavenumbers. The dispersion diagram in Fig. 2(a) shows a good match between the real value of the space-charge wavenumber calculated based on the proposed method (based on Eq. 8) and the one calculated based on Branch and Mihran's method [6] (which is real-valued). We show in Fig. 2(b) the ‘‘PIC-based’’ reduction factor calculated as in (9).

We now compare the PIC-based result obtained from the method described above with the analytical one based on Branch and Mihran's work in [6]. According to that theory, the plasma frequency reduction factor is approximated as

$$R_{\text{Theory}} = \frac{1}{\sqrt{1 + (T/\beta_0)^2}}, \quad (10)$$

where $\beta_0 = \omega/u_0$ is the mean electronic phase constant and the parameter T is found by solving the following nonlinear equation [5], [6]

$$T R_b \frac{J_1(T R_b)}{J_0(T R_b)} = \beta_0 \frac{K_0(\beta_0 R_t) I_1(\beta_0 R_b) + K_1(\beta_0 R_b) I_0(\beta_0 R_t)}{K_0(\beta_0 R_b) I_0(\beta_0 R_t) - K_0(\beta_0 R_t) I_0(\beta_0 R_b)}, \quad (11)$$

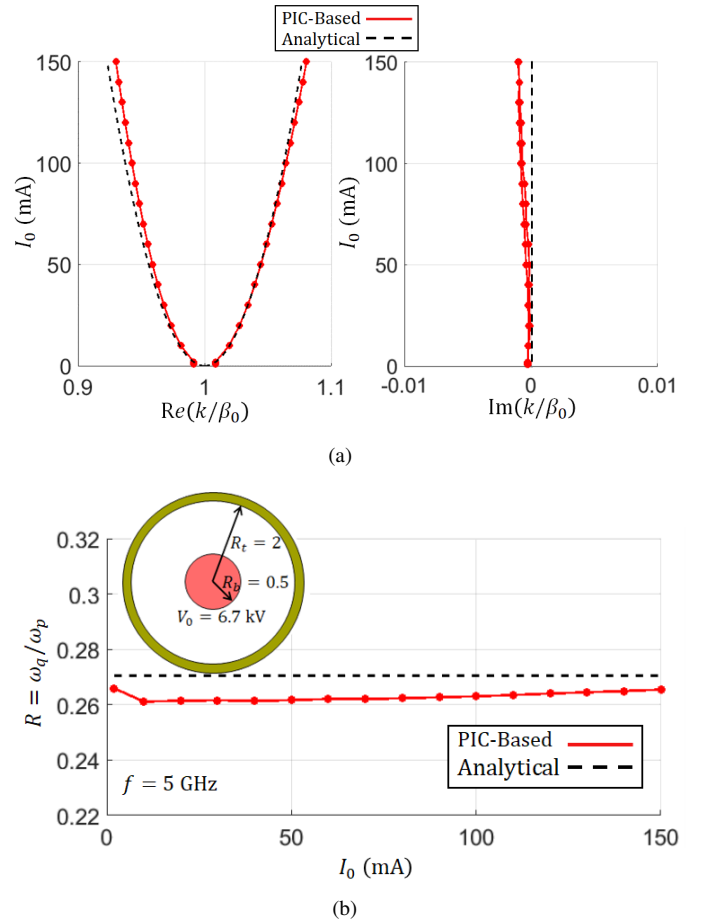


Fig. 2. (a) Dispersion relation showing the wavenumbers of the eigenmodes of the space-charge wave supported by the electron beam. Dimensions are shown in the inset of (b), with units of mm. The proposed PIC-based method is compared with the analytical results from Branch and Mihran [6]. (b) Corresponding plasma frequency reduction factor versus beam current. Our results are in agreement with the analytical ones in (10) and (11), that show that the plasma frequency reduction factor is current independent.

where the various orders and kinds of Bessel functions are defined in [6]. The two real-valued wavenumbers $k_1 = \beta_0 - \omega_q/u_0$ and $k_2 = \beta_0 + \omega_q/u_0$ based on Branch and Mihran's method [6], where $\omega_q = R_{\text{Theory}}\omega_p$, are plotted in Fig. 2(a), as ‘‘Analytical’’, and the reduction factor R_{Theory} is shown in Fig. 2(b). Note that from (10) and (11), the reduction factor is independent of the beam current value I_0 . However, the unreduced plasma frequency and the two wavenumbers are all dependent on beam current. As expected, the reduction factor obtained by the proposed PIC-based method seems to be almost constant when varying the beam dc current. The results show a good match between the plasma frequency reduction factor obtained based on PIC simulations and that based on theoretical formulas in (10) and (11), with a maximum absolute error in R of 0.01, which is very small with respect to the reduction factor obtained theoretically. Note that when $I_0 \rightarrow 0$, the plasma frequency $\omega_p \rightarrow 0$ and therefore the two space-charge waves have wavenumbers $k_1 = k_2 = \beta_0$ as illustrated in Fig 2(a). The dispersion relation around $I_0 = 0$ can be

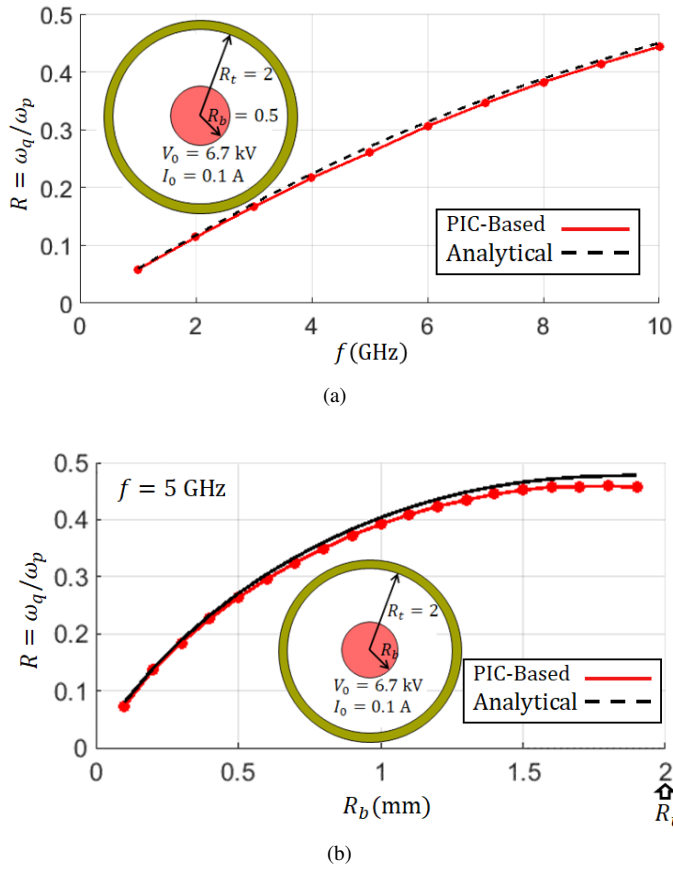


Fig. 3. Reduction factor calculated for a cylindrical beam in a metallic tunnel with geometry as shown in the insets, when (a) the frequency is swept, and (b) the beam radius is swept. The dimensions shown in the insets are in mm.

approximated to a quadratic polynomial as $(k - \beta_0)^2 \propto I_0$ as illustrated in Fig 2(a), and this has a deep physical meaning as it will be discussed later on. We show in Fig. 3(a) and Fig. 3(b) the plasma frequency reduction factor when the frequency is swept at constant beam dc current of $I_0 = 100$ mA, and when the beam radius is swept at constant dc current $I_0 = 100$ mA and frequency $f = 5$ GHz, respectively. The agreement between the PIC-based solution provided in this paper and the analytical one from (10) and (11) is excellent.

IV. DEGENERACY OF THE SPECTRUM

To provide a physical insight into the result, it is convenient to analyze the spectral properties of the system matrix \mathbf{M} that describes the system as in (3). Following the space-charge wave theory in [2] and also using the formulation presented in [30], we use the analytically determined matrix

$$\mathbf{M}_{\text{Theory}} = \begin{bmatrix} \beta_0 & \frac{R_{\text{Theory}}^2}{(A\omega\epsilon_0)} \\ \beta_p^2 (A\omega\epsilon_0) & \beta_0 \end{bmatrix}, \quad (12)$$

where $\beta_p = \omega_p/u_0$ is the unreduced plasma phase constant, and the reduction factor R_{Theory} is taken from (10). The theoretical wavenumbers of the space-charge waves are found as the eigenvalues of the system matrix $\mathbf{M}_{\text{Theory}}$, $k_1 = \beta_0 - \omega_q/u_0$ and $k_2 = \beta_0 + \omega_q/u_0$ which agree with the

space-charge wavenumber expressions found in [5], [6], [8], and correspond to those already plotted in Fig. 2(a). The ac electron kinetic energy and the ac beam current of the two space-charge waves are described by the two eigenvectors of the matrix (12) as $\Psi_1 = [-R_{\text{Theory}}/(\beta_p A\omega\epsilon_0), 1]^T$ and $\Psi_2 = [R_{\text{Theory}}/(\beta_p A\omega\epsilon_0), 1]^T$.

We know that when two eigenvectors coalesce, the system experiences an exceptional point of degeneracy (EPD) of order 2, where the system matrix is not diagonalizable and is instead similar to a Jordan block of order 2, as explained in [30]–[33]. Therefore, the eigenmodes experience an algebraic linear behavior, besides the usual phase propagation along z . At an EPD where the space charge waves are degenerate (i.e., when $k_1 = k_2 = \beta_0$), the beam ac voltage is expressed as $V_b(z) = (u_1 + u_2 z)e^{-j\beta_0 z}$, whereas away from the EPD, it is expressed as $V_b(z) = e^{-j\beta_0 z}(u_1 e^{-j\beta_q z} + u_2 e^{j\beta_q z})$. The point $I_0 = 0$ in Fig. 2(a) represents an EPD, and indeed, in its proximity the two wavenumbers follow the law $(k - \beta_0)^2 \propto I_0$. A vanishing I_0 indicates the absence of the beam but one can still see the physics pertaining to an EPD at regimes where I_0 is very small. The two eigenvectors also coalesce when the reduction factor R is very small, hence the system can experience an EPD at $R = 0$. It is convenient to use a “coalescence parameter” that quantifies the vicinity of the two eigenvectors to each other (i.e., to describe how close is a system’s regime to an EPD). To check the coalescence parameter, we look at the angle between the two system’s two eigenvectors, when the current elements are scaled by an impedance of $Z_0 = \beta_0/(A\omega\epsilon_0)$ to have vectors that have all elements in volts, (that is defined by the normalized scalar product as $\cos\theta_{12} = \text{Re}(\Psi_1 \cdot \Psi_2) / (\|\Psi_1\| \|\Psi_2\|)$). The coalescence parameter is here calculated as

$$\sin(\theta_{12}) = \frac{2R \left(\frac{\omega_p}{\omega} \right)}{1 + R^2 \left(\frac{\omega_p}{\omega} \right)^2}, \quad (13)$$

and it describes how close the two eigenvectors of the system are to coalescing (i.e., when the system experiences an EPD), which occurs when $\sin\theta_{12} = 0$, i.e., when either $R = 0$ or $\omega_p = 0$. Indeed, in regimes where the plasma frequency is very small with respect to the operating frequency, the system is very close to an EPD. We show in Fig. IV the space-charge wave behavior when the system is very close to EPD, i.e., for a case where the plasma frequency is $f_p = 0.11$ GHz and the operating frequency $f = 5$ GHz, where a beam dc current $I_0 = 1$ mA is used. The ac beam equivalent voltage and current decays and grows, respectively, linearly, along z . This behavior is different from other cases where the EPD does not occur, as shown in Fig. 1(b) for example.

V. CONCLUSION

A method to determine the reduction factor for single stream electron beam flowing inside of a tunnel has been demonstrated using a novel technique. Our method is based on analyzing the data obtained from time-domain 3D PIC

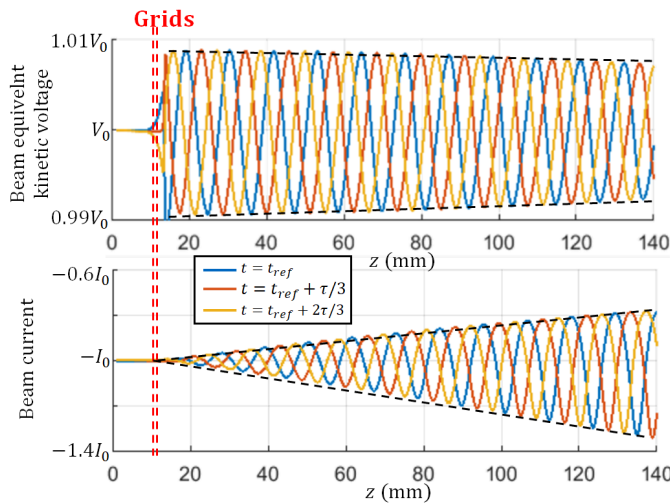


Fig. 4. An example of electron beam dynamics when the system is very close to an EPD. The distribution of the electron beam total equivalent kinetic voltage and current decays and grows algebraically, respectively, along the z direction.

simulations, hence it accounts for all the physical aspects of the problem. Our model is general and can be applied to several other geometries supporting electron beams that are different from the one used here for demonstration purposes. The proposed method seems precise since the calculated reduction factor is in good agreement with the one obtained analytically for cylindrically-shaped electron beam flowing inside a cylindrical metallic tunnel [6]. Since the proposed method is just based on 3D PIC simulations, it can be utilized to study electron beams in complex-shaped beam tunnels, where no theoretical model yet exists, or even for electron beams made of multiple streams as in [21]–[23].

ACKNOWLEDGMENT

The authors are thankful to DS SIMULIA for providing CST Studio Suite that was instrumental in this study.

REFERENCES

- [1] L. Tonks and I. Langmuir, "Oscillations in ionized gases," *Physical Review*, vol. 33, no. 2, p. 195, 1929.
- [2] S. E. Tsimring, "Klystrons," in *Electron beams and microwave vacuum electronics*, ch. 7, pp. 263–296, Hoboken, NJ, USA: John Wiley & Sons, 2007.
- [3] A. Gilmour, *Klystrons, traveling wave tubes, magnetrons, crossed-field amplifiers, and gyrotrons*. Norwood, MA, USA: Artech House, 2011.
- [4] W. Hahn, "Small signal theory of velocity-modulated electron beams," *Gen. Elec. Rev.*, vol. 42, no. 6, pp. 258–270, 1939.
- [5] S. Ramo, "Space charge and field waves in an electron beam," *Physical Review*, vol. 56, no. 3, p. 276, 1939.
- [6] G. Branch and T. Mihran, "Plasma frequency reduction factors in electron beams," *IRE Transactions on Electron Devices*, vol. 2, no. 2, pp. 3–11, 1955.
- [7] J. W. Gewartowski and H. A. Watson, *Principles of electron tubes*. New York, NY, USA: Van Nostrand, 1965.
- [8] S. K. Datta and L. Kumar, "A simple closed-form formula for plasma-frequency reduction factor for a solid cylindrical electron beam," *IEEE transactions on electron devices*, vol. 56, no. 6, pp. 1344–1346, 2009.
- [9] T. Antonsen and B. Levush, "Traveling-wave tube devices with nonlinear dielectric elements," *IEEE transactions on plasma science*, vol. 26, no. 3, pp. 774–786, 1998.
- [10] J. R. Pierce, "Traveling-wave tubes," *The bell System technical journal*, vol. 29, no. 2, pp. 189–250, 1950.
- [11] T. M. Antonsen Jr and B. Levush, "Christine: A multifrequency parametric simulation code for traveling wave tube amplifiers," tech. rep., Naval Research Lab, Washington, DC, USA, 1997.
- [12] J. G. Wohlbiert, J. H. Booske, and I. Dobson, "The multifrequency spectral eulerian (muse) model of a traveling wave tube," *IEEE Transactions on Plasma Science*, vol. 30, no. 3, pp. 1063–1075, 2002.
- [13] P. Tien, L. Walker, and V. Wolontis, "A large signal theory or traveling-wave amplifiers," *Proceedings of the IRE*, vol. 43, no. 3, pp. 260–277, 1955.
- [14] D. H. Simon, P. Wong, D. Chernin, Y. Lau, B. Hoff, P. Zhang, C. Dong, and R. M. Gilgenbach, "On the evaluation of pierce parameters c and q in a traveling wave tube," *Physics of Plasmas*, vol. 24, no. 3, p. 033114, 2017.
- [15] P. Wong, P. Zhang, and J. Luginsland, "Recent theory of traveling-wave tubes: a tutorial-review," *Plasma Research Express*, vol. 2, no. 2, p. 023001, 2020.
- [16] G. Branch, T. Mihran, W. Neugebauer, and W. Pohl, "Space-charge wavelengths in electron beams," *IEEE Transactions on Electron Devices*, vol. 14, no. 7, pp. 350–357, 1967.
- [17] G. Vorob'ev, A. Y. Kirichenko, A. Tsvyk, and L. Tsvyk, "Experimental determination of reduced plasma frequency of an electron flux," *Radio-physics and quantum electronics*, vol. 33, no. 10, pp. 854–859, 1990.
- [18] T. Mealy and F. Capolino, "Traveling wave tube eigenmode solution for beam-loaded slow wave structure based on particle-in-cell simulations," *IEEE Transactions on Plasma Science*, vol. 50, no. 3, pp. 635–648, 2022.
- [19] J. Pierce, "Double-stream amplifiers," *Proceedings of the IRE*, vol. 37, no. 9, pp. 980–985, 1949.
- [20] J. R. Pierce and W. B. Hebenstreit, "A new type of high-frequency amplifier," *The Bell System Technical Journal*, vol. 28, no. 1, pp. 33–51, 1949.
- [21] A. Figotin, "Multi-stream e-beam," in *An Analytic Theory of Multi-stream Electron Beams in Traveling Wave Tubes*, ch. 48, pp. 335–341, Singapore: World Scientific, 2021.
- [22] K. N. Islam, L. Ludeking, A. D. Andreev, S. Portillo, A. M. Elfrgani, and E. Schamiloglu, "Modeling and simulation of relativistic multiple electron beam generation with different energies from a single-cathode potential for high-power microwave sources," *IEEE Transactions on Electron Devices*, vol. 69, no. 3, pp. 1380–1388, 2022.
- [23] K. Islam and E. Schamiloglu, "Multiple electron beam generation with different energies and comparable currents from a single cathode potential for high power traveling wave tubes (twts)," *Journal of Applied Physics*, vol. 131, no. 4, p. 044901, 2022.
- [24] C. K. Birdsall, G. R. Brewer, and A. V. Haeff, "The resistive-wall amplifier," *Proceedings of the IRE*, vol. 41, no. 7, pp. 865–875, 1953.
- [25] T. Rowe, N. Behdad, and J. H. Booske, "Metamaterial-enhanced resistive wall amplifier design using periodically spaced inductive meandered lines," *IEEE Transactions on Plasma Science*, vol. 44, no. 10, pp. 2476–2484, 2016.
- [26] T. Rowe, J. H. Booske, and N. Behdad, "Metamaterial-enhanced resistive wall amplifiers: Theory and particle-in-cell simulations," *IEEE Transactions on Plasma Science*, vol. 43, no. 7, pp. 2123–2131, 2015.
- [27] P. Forbes, N. Behdad, and J. H. Booske, "Effective-medium modeling of a meanderline metamaterial-enhanced resistive wall amplifier circuit for particle-in-cell simulations," *IEEE Transactions on Plasma Science*, vol. 49, no. 9, pp. 2700–2708, 2021.
- [28] G. Williams, "Overdetermined systems of linear equations," *The American Mathematical Monthly*, vol. 97, no. 6, pp. 511–513, 1990.
- [29] H. Anton and C. Rorres, "General vector spaces," in *Elementary linear algebra: applications version*, ch. 4, pp. 183–290, Hoboken, NJ, USA: John Wiley & Sons, 2013.
- [30] K. Rouhi, R. Marosi, T. Mealy, A. F. Abdelshafy, A. Figotin, and F. Capolino, "Exceptional degeneracies in traveling wave tubes with dispersive slow-wave structure including space-charge effect," *Applied Physics Letters*, vol. 118, no. 26, p. 263506, 2021.
- [31] T. Mealy, A. F. Abdelshafy, and F. Capolino, "Exceptional point of degeneracy in a backward-wave oscillator with distributed power extraction," *Physical Review Applied*, vol. 14, no. 1, p. 014078, 2020.
- [32] A. Figotin, "Exceptional points of degeneracy in traveling wave tubes," *Journal of Mathematical Physics*, vol. 62, no. 8, p. 082701, 2021.

- [33] T. Kato, "Perturbation theory in a finite-dimensional space," in *Perturbation theory for linear operators*, ch. 2, pp. 62–126, New York: Springer-Verlag New York Inc., 1966.